

## FRAGILITY FUNCTION OF BURIED PIPELINES UNDER HIGH LEVEL OF GROUND MOTION WITH THE AID OF DEM ANALYSIS

S. Takada<sup>1</sup>, Y. Kuwata<sup>2</sup> and Y. Tanaka<sup>3</sup>

<sup>1</sup> Emeritus Professor, Dept. of Civil Engineering, Kobe University, Kobe, Japan

<sup>2</sup> Associate Professor, Dept. of Civil Engineering, Kobe University, Kobe, Japan

<sup>3</sup> Graduate Student, Dept. of Civil Engineering, Kobe University, Kobe, Japan

Email: takada@kobe-u.ac.jp

### ABSTRACT :

Seismic damage estimation for buried pipeline has been done by using damage estimation formulae (fragility function) obtained by statistical data in the past earthquakes. However these functions are reliable up to the level of ground motion which is used for the development of formula. Moreover any theoretical or numerical calculation for the pipeline damage formulae does not exist. Here we propose a new method to obtain fragility functions of buried pipelines depending on the failure modes by applying a numerical simulation of DEM, which are compared with the past fragility functions.

**KEYWORDS:** fragility function, buried pipeline, high level ground motion, DEM analysis, pipe joint

### 1. INTRODUCTION

Seismic damage estimation for buried pipeline has been done by using damage estimation formulae (so called, fragility function) obtained by statistical data in the past earthquakes. Isoyama et al.(1998) proposed a fragility function for DIP and CIP pipelines based on the data during the 1995 Kobe earthquake, which shows the pipe damage is exponentially increase according to ground velocity. Hosokawa et al. (2001) also proposed a fragility function which shows that the damage ratio of low pressure gas pipelines reaches to be constant when the ground motion becomes more than 100kine.

However, any theoretical or numerical calculation for the pipeline damage formulae does not exist so far. Also, the fragility function has been obtained for the level of ground motions less than 100kine. Recent ground motion records show the higher level of ground motion than 100kine. Here we propose a new method to obtain fragility functions of buried pipelines depending on the failure modes by applying a numerical simulation of DEM, which are compared with the past fragility functions.

### 2. ANALYTICAL METHOD BY DEM

#### 2.1. Model of pipeline

DEM is an analytical method to treat the motion of a set of particles as the non-continuous media. Three dimensional equilibrium equations can be shown as follows:

$$\ddot{x}_i + \alpha \dot{x}_i = F_i / m_i + g \quad (2.1)$$

$$\dot{\omega}_i + \alpha \omega_i = M_i / I_i \quad (2.2)$$

Where,  $x_i$  : coordinate of particle,  $\alpha$  : damping constant,  $F_i$  : total force acting to particle,  $m_i$  : mass of particle  $i$ ,  $g$  : gravity,  $\omega_i$  : rotation velocity of particle,  $M_i$  : total moment of particle,  $I_i$  : Inertia moment of particle  $i$ .

Figure 2.1 shows a model of pipeline under the ground by DFM. Pipe is modeled by concentrated mass and beam and pipe joint is expressed by specific spring between two particles, which allows three dimensional behavior. Soil spring means the restrained force with slippage between pipe and ground. Figure 2.2 is a targeted straight pipeline model with 100m length of  $\Phi 100$  and 150mm. One segment of the pipeline is 4 and 5m for  $\Phi 100$  and  $\Phi 150$ mm diameter pipeline respectively. The end of the pipeline is set to free conditions to avoid stress concentrations. Materials of the pipe are DIP (Ductile iron pipe), CIP (Cast iron pipe) and PVC (Polyvinyl pipe), whose features are listed in Table 2.1. Bending characteristics for DIP and CIP are determined in terms of  $EI$ . For PVC, M- $\Phi$  relations are introduced as shown in Figure 2.3. Soil spring is set referred to JGA specification (1996) as listed in Table 2.2.

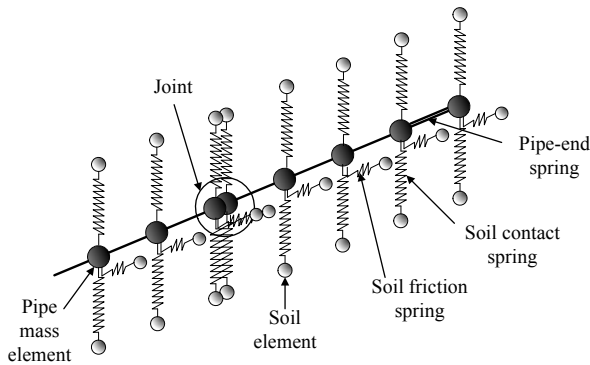


Figure 2.1 Pipeline model by DEM

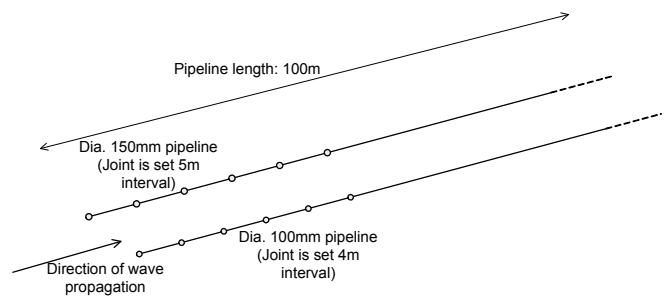


Figure 2.2 Analytical model of pipeline

Table 2.1 Features of targeted pipes

| Pipe | N.Diameter (mm) | Diameter (mm) | $t$ (mm) | $E$ (N/mm <sup>2</sup> ) | $\sigma_t$ (N/mm <sup>2</sup> ) | $\sigma_c$ (N/mm <sup>2</sup> ) |
|------|-----------------|---------------|----------|--------------------------|---------------------------------|---------------------------------|
| DIP  | 100             | 118           | 6        | 157,000                  | 420                             | 840                             |
|      | 150             | 169           | 6        |                          |                                 |                                 |
| CIP  | 100             | 114           | 4.5      | 155,000                  | 200                             | 730                             |
|      | 150             | 159           | 4.5      |                          |                                 |                                 |
| PVC  | 100             | 114           | 7.1      | 2,700                    | 52                              | 65                              |
|      | 150             | 165           | 9.6      |                          |                                 |                                 |

Table 2.2 Soil spring features

| Pipe | Soil spring $k$ (N/cm <sup>3</sup> ) |       | Yield Displ.(cm) |
|------|--------------------------------------|-------|------------------|
|      | Transverse                           | Axial |                  |
| DIP  | 13.1                                 | 5.9   | 0.5              |
| CIP  | 13.5                                 | 5.9   | 0.5              |
| PVC  | 13.5                                 | 2.9   | 0.5              |

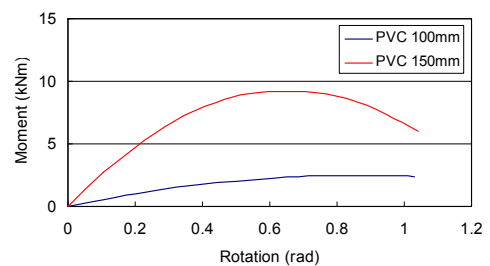


Figure 2.3 PVC Bending characteristics

### 2.2 Pipe joint models

A, K and T-types of DIP pipelines (Figure 2.4) are analyzed. Damage of these pipelines is defined as the state where displacement or rotation angle of the joints reaches to the ultimate values due to ground motions.

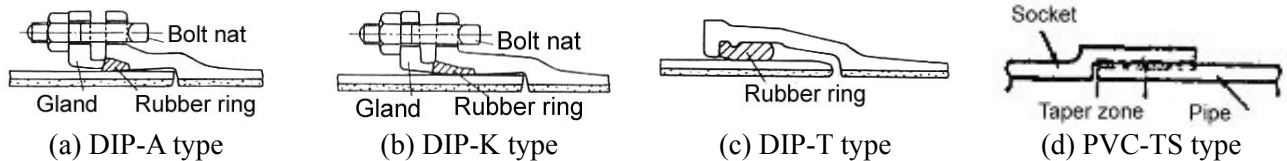


Figure 2.4 Pipe joint (JWWA, 1997)

Figure 2.5 shows the ultimate tension and compression displacements and also rotation angle in each type of DIP joint.

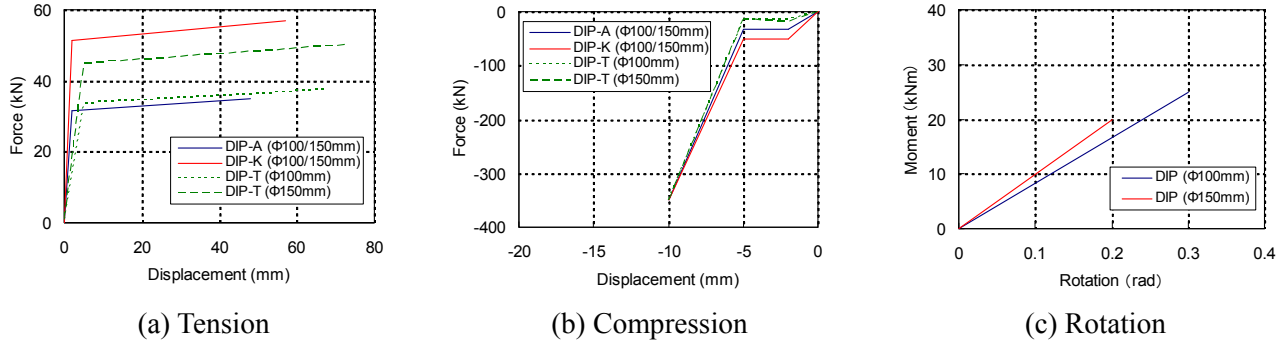


Figure 2.5 DIP Joint characteristics for A, K and T types

The joint characteristics of CIP are obtained by experiments for gas CIP pipes. These joint behaviors are shown in Figure 2.6 along with the joint characteristics of PVC-TS joint.

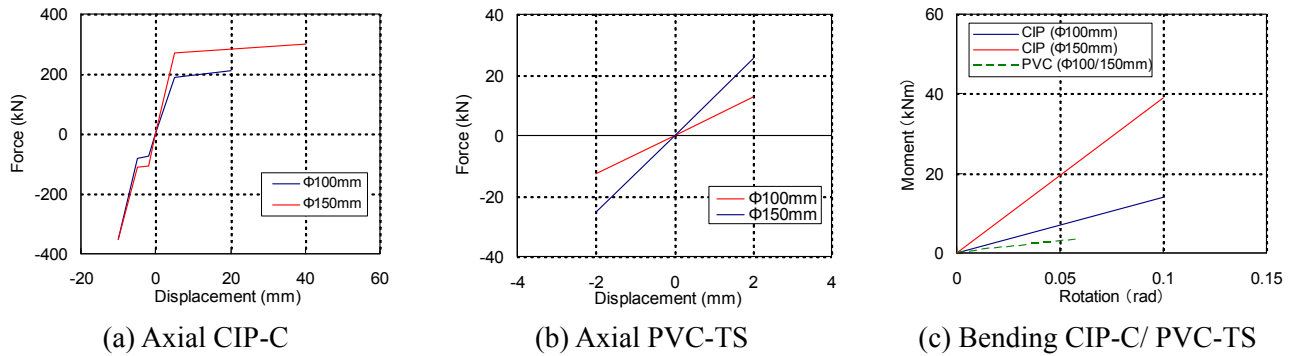


Figure 2.6 Joint characteristics for CIP-C and PVC-TS

### 2.3 Input ground motions

In the seismic response analyses by DEM, the accelerogram of strong ground motion observed at Takatori station is used for the input ground motions, which has a predominant period of about 1.0second. The velocity amplitude of the records is converted to 8 levels to check the change of response behavior.

## 3. ANALITICAL RESULT

### 3.1 Comparison of theoretical and numerical response value for joint displacement

In the numerical analyses, a phase difference of the input ground motions is given by making the input ground motions propagate by a variable speed  $C$ . On the other hand, a theoretical ground strain and joint displacement can be calculated as follows.

$$\varepsilon_{soil} = \varepsilon_{pipe} = \frac{V_{max}}{C} \quad (3.1)$$

where,  $\varepsilon_{soil}$  : ground strain,  $\varepsilon_{pipe}$  : pipe strain,  $V_{max}$ : maximum velocity (120cm/s),  $C$ : wave speed (cm/s)

$$\Delta j = L_p \cdot \varepsilon_{soil} \quad (3.2)$$

where,  $\Delta j$  : joint displacement (cm),  $L_p$ : pipe length (in case of 400cm),

Figure 3.1 shows the compared results, which indicate a fairly good agreement under high level of ground motions. The compressive displacement at every joint is over an allowable compressive displacement of the joint, which means the joints have high rigidity due to collision in adjacent pipe segments and some joints have pull out behavior under low speed wave propagation, though both results do not give large difference. Then we have to check the behavior not only average value of the joints, but the behavior of each joint.

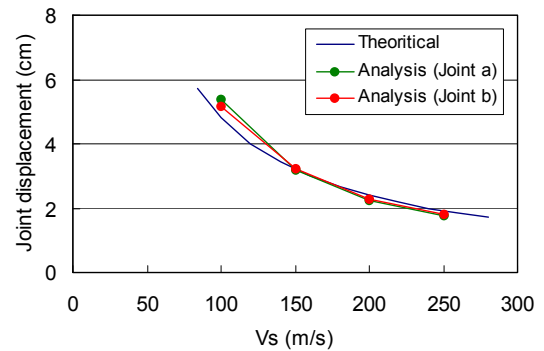


Figure 3.1 Comparison of theory and numerical results (120kine)

### 3.2 Fragility curves of joint and body

Fragility ratio of joints depending on the maximum ground velocity  $F_r(V_{max})$  is defined by,

$$F_r(V_{max}) = \frac{J_f}{J} \times 100 \quad (3.3)$$

Here,  $F_r$ : fragility ratio (%),  $J_f$ : number of failure joint,  $J$ : total number of joint

The relation between the maximum ground velocity  $V_{max}$  and  $F_r(V_{max})$  gives fragility function for each pipeline. Figure 3.2 shows fragility function for various types of joint of DIP, CIP and PVC. For the smaller amplitude of ground velocity less than 120kine, DIP-T type joint has less damage ratio due to larger allowable expansion displacement of 67mm. For larger velocity amplitude of 150kine, the joints with higher rigidity have less damage ratio. PVC-TS type pipe is subjected to breakage in every joint location. Figure 3.3 shows the fragility functions for  $\Phi 150$  mm pipelines. The tendency of damage ratio for each type of joints is much difference compared with  $\Phi 100$ mm pipelines shown in Figure 3.2. CIP shows low reliability from the smaller velocity amplitude of ground. Velocity amplitude is just 10kine when the CIP joint starts to be broken, whereas PVC-TS type starts to be broken at 30kine. The larger diameter pipe has easiness to be broken in compressive behavior compared with smaller diameter pipelines due to joint characteristics.

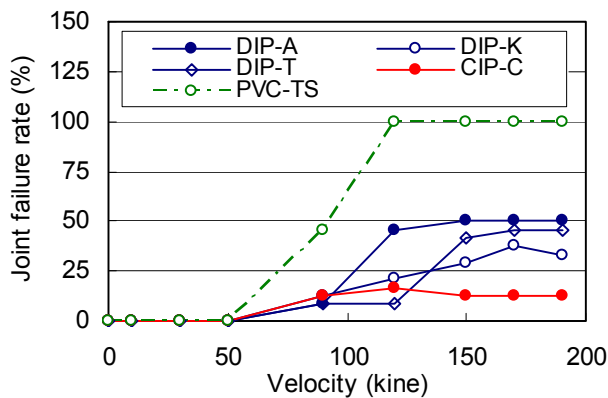


Figure 3.2 Fragility for pipe body ( $\Phi 100$ mm)

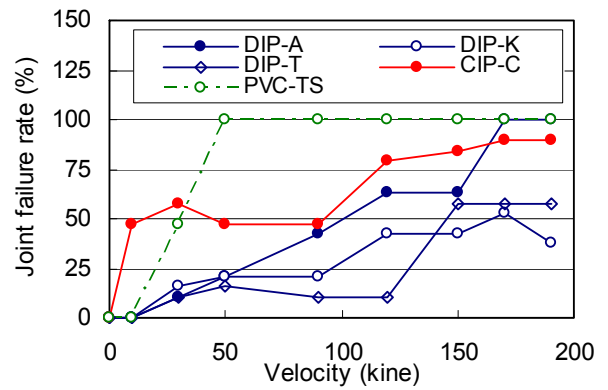


Figure 3.3 Fragility for pipe joint ( $\Phi 150$ mm)

### 3.3 Maximum axial force

Figures 3.4 and 3.5 show the relation between ground velocity amplitude and maximum axial force in the pipelines. The maximum axial force shows its peak value almost at 50kine and does not increase more for larger amplitude in every type of pipelines. The pipeline resists to ground motions by pipe displacement for tension force and by joint rigidity for compressive forces. Then these maximum axial forces are corresponding to compressive forces. Pulling out of DIP-T type pipeline causes the decrease of axial forces at 90kine.

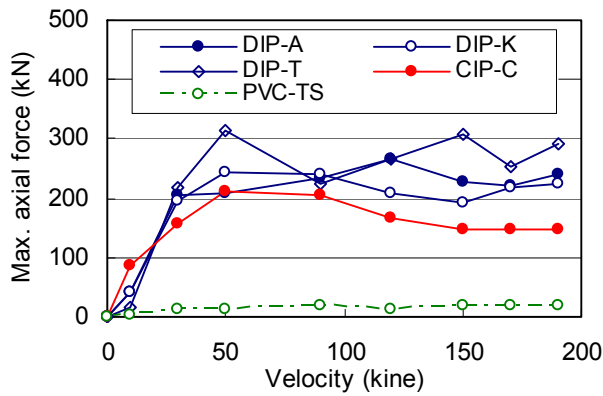


Figure 3.4 Maximum axial force (Φ100mm)

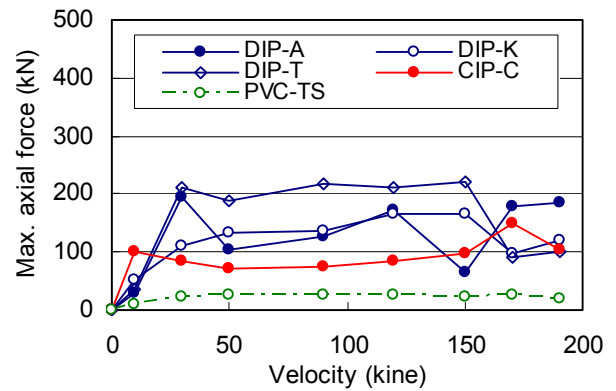


Figure 3.5 Maximum axial force (Φ150mm)

### 3.4 Fragility curves of pipelines

We have discussed on the damage of pipe joint and body separately in the above explanation. Next, fragility function of pipeline (pipe fragility function) is defined as an averaged value of the joint damage ratio and ratio of the axial force to allowable axial force of pipe body. Figures 3.6 and 3.7 show the pipe fragility functions related with ground velocity. The pipe fragility function shows the tendency of constant values for higher level of ground amplitude, which is harmony with the actual damage during the Kobe earthquake as Takada et al. (2001) and JWWA (1996).

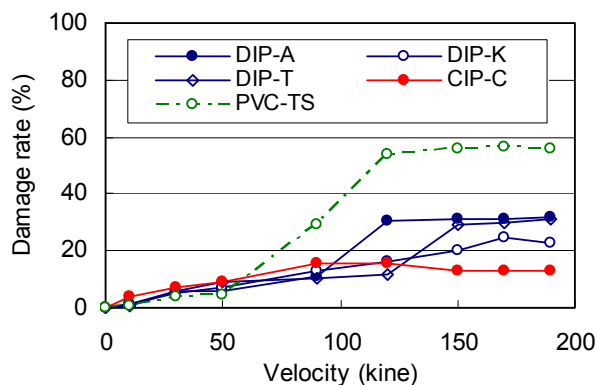


Figure 3.6 Pipe fragility function (Φ100mm)

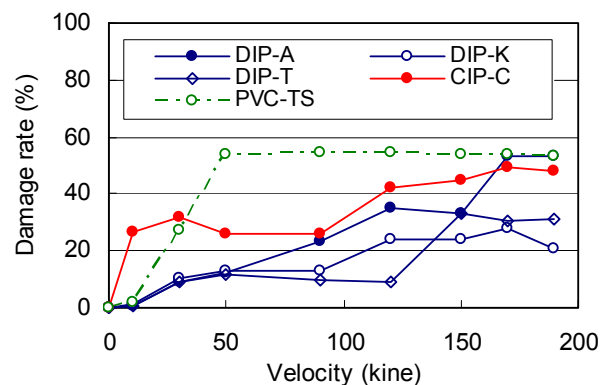


Figure 3.7 Pipe fragility function (Φ150mm)

## 4. CONCLUSIONS

Obtained results would be somewhat changed under the assumed parameters in DEM analyses. However, it becomes clear that we can evaluate the pipe fragility function numerically even in the meaning of relative evaluation by giving pipe material and joint characteristics. Moreover, this study has revealed that the pipeline failure under high level of ground motions is the discontinuous damage process of joints and the pipe fragility function becomes constant due to the limitation of the axial force applied to pipeline.

Followings are the results obtained by present numerical calculations.

- 1) Expansion and compressive behavior of pipe joints strongly depends on the ground strain. Numerical calculation results for pipe joint displacements are mostly proportional to theoretical results. However, numerical calculation results show higher value than theoretical ones due to complicated joint behavior in each other.
- 2) Proposed DEM can make clear the behavior of buried pipelines even under high level of ground motions, which can not done by using past earthquake damage data. Diameter of pipes and joint characteristics give

important effects to pipe fragility functions. Generally speaking, DIP-A, DIP-K and DIP-T have less seismic reliability in order and CIP is the most vulnerable pipe material.

- 3) The pipeline resists to the ground motions by pipe displacement for tension force and by joint rigidity for compressive forces. Then these maximum axial forces are corresponding to compressive forces.
- 4) The pipeline failure under high level of ground motions is the discontinuous damage process of joints and the pipe fragility function becomes constant due to the limitation of the axial force applied to pipeline.

## REFERENCES

- Hosokawa, N., Watanabe, T., Shimizu, Y., Koganemaru, K. Ogawa, Y., Kitano, T., Isoyama, R. (2001). Damage estimation formula for low pressure gas pipelines considering ground conditions under large scale earthquake, *Proceedings of the JSCE 26<sup>th</sup> Earthquake Engineering Symposium*, 1333-1336.
- Isoyama, R., Ishida, E., Yune, K., Shirozu, T. (1998). Seismic damage estimation procedure for water pipes, *10<sup>th</sup> Japan Symposium on Earthquake Engineering*, 3175-3180.
- Japan Gas Association. (1982). *Seismic design guideline for gas pipelines*.
- Japan Water Works Association. (1997). *Seismic design guideline and commentary*.
- Japan Water Works Association. (1996). *Damage and analysis of water pipelines at the 1995 Hyogo-ken Nanbu earthquake*.
- Takada, S., Ivanov, R., Morita, N. (2003). Large deformation analysis of jointed pipelines by DEM, *Memoirs of Construction Engineering Research Institute Foundation*, **45**, 111-122.
- Takada, S., Miyajima, M., Yoda, M., Fujiwara, M., Suzuki, Y., Toshima, T. (2001). Study on the damage prediction method of buried pipelines under near field earthquake disaster, *JWWA journal*, **798**, 21-37.